UDC 551.521.14:551.507.362.2:551.576(084.1)"1967.02-1968.02"

THE ANNUAL COURSE OF ZONAL MEAN ALBEDO AS DERIVED FROM ESSA 3 AND 5 DIGITIZED PICTURE DATA

JAY S. WINSTON

National Environmental Satellite Service, NOAA, Washington, D.C.

ABSTRACT

Temporal and meridional variations of zonal means of albedo and absorbed solar radiation, derived from digitized satellite pictures, are portrayed for the period February 1967–February 1968 over a broad range of latitudes. The variations in a number of prominent features of the zonal mean albedo—the maxima associated with the intertropical convergence zone, the minima associated with the subtropical anticyclones and equatorial dry zone, and the poleward ascendants of albedo from the subtropics—are revealed in more detail than possible heretofore. The annual courses of zonal mean albedo in three component sectors of 120° longitude each are also shown. The sector covering the zone 0°–115°E differs the most from the overall mean and from the other two sectors covering the Pacific and Atlantic-Americas regions. These differences are most pronounced in the period June–August when the summer monsoon is dominant over Southeast Asia.

Harmonic analysis of the overall zonal mean albedo values for a full year at individual latitude circles between 0° and 45°N indicates the relative prominence of the annual, semiannual, and other long-period oscillations at the various latitudes. The annual cycle is dominant in latitudes 25°–45°N and 10°–15°N. At 0°, 5°, and 20°N, the semiannual cycle is stronger than the annual cycle. In the Tropics and subtropics, amplitudes of frequencies corresponding to periods of 28–30 days are more prominent than all but the very long-period oscillations (i.e., 90–365 days).

The annual course of the absorbed solar radiation associated with these albedo values exhibits some interesting features brought about by the asymmetries of albedo in the Northern Hemisphere relative to the equinoxes and summer solstice. For example, the consistently higher albedos at all latitudes northward of 20°N and lower values at 10°–15°N in March than in September result in a poleward gradient of absorbed solar radiation considerably stronger at the vernal than at the autumnal equinox. Comparison of albedos and absorbed solar radiation for Northern and Southern Hemispheres near their respective summer solstices reveals that the poleward ascendant of albedo is much stronger in the Southern Hemisphere and that, therefore, the poleward gradient of absorbed solar radiation is considerably stronger too.

1. INTRODUCTION

The archive of digitized brightness values derived from the advanced vidicon camera system on the odd-numbered ESSA satellites (i.e., ESSA 3, 5, 7, 9) and ITOS 1 since the beginning of 1967 constitutes the most comprehensive record, both in space and time, of the solar energy reflected from the earth-atmosphere system. Pictorial and digital presentations of these data, both on an individual daily basis and in terms of time averages, have already appeared frequently in the literature (e.g., Taylor and Winston 1968, Booth and Taylor 1969, Kornfield and Hasler 1969). In addition, daily and time-averaged composites of these digitized pictures have been assembled in motion pictures [1] to portray time variations of (principally) cloudiness.

The present study is concerned with time variations of zonal averages of albedo and absorbed solar radiation derived from these brightness data over the course of more than a year (February 1967 through February 1968). The principal characteristics of the temporal and meridional variations of the zonally averaged reflected and absorbed solar energy are exhibited by means of time-latitude charts of 6-day mean values and by harmonic analysis of daily values.

[1] Available from Walter A. Bohan Co., Park Ridge, Ill.

Previous analyses of zonally averaged albedo and absorbed solar radiation obtained from satellite measurements have been confined to seasonal and monthly mean values (e.g., Bandeen et al. 1965, Rasool and Prabhakara 1966, Vonder Haar 1968, Winston 1969, Raschke and Bandeen 1970). Furthermore, most of these averages were taken over substantial spatial and temporal gaps in the data. The Nimbus II albedo data (Raschke and Bandeen 1970) probably suffered the least in regard to such data gaps, but unfortunately the data were obtained over a period of only 2 1/2 months.

The special asset of the brightness data is that for the first time there is a record of more than a year of virtually complete data coverage over entire latitude circles northward from the equator, except over the poorly illuminated high latitudes in the period centered about the winter solstice. The Southern Hemisphere was similarly well observed except during June through mid-September 1967 when ESSA 5 was observing too late in the afternoon to allow for a sufficient response by the camera over the entire area of each picture. Aside from this one substantial gap, only a relatively few days of data were missing from the period studied. Thus quite representative medium-period (i.e., 6-day) means could be constructed and only a modest amount of interpolation of missing data was needed to form a complete daily record

over much of the Northern Hemisphere for harmonic analysis.

2. DATA USED AND DERIVATION OF ALBEDO FROM BRIGHTNESS

The zonally averaged data studied here were obtained from daily brightness values averaged in 5° latitude-longitude squares centered at the 5° latitude-longitude intersections. These 5° averages in turn were derived from the mesoscale archival tape.[2] (See Bristor et al. 1966 and Bristor 1968 for details of the digitization procedure and production of this mesoscale archive.) The daily values at the 5° latitude-longitude intersections, averaged directly from the archive, still showed variations with time at certain check points over the earth under apparently cloudless conditions. These shifts in brightness over places where little change in brightness would be expected were found to correspond to camera changes (two aboard each satellite used alternately) in some cases, but there were also some cases of degradation in camera response apparently associated with changes in spacecraft temperature (Schwalb and Gross 1969). Very simple empirical corrections were made in the data to compensate for such changes, thereby making the complete record of data relatively homogeneous. These adjustments and other details of the construction of daily maps using the 5° latitude-longitude grid are discussed by Taylor and Winston (1968).

Since a purpose of the present study is to obtain estimates of first reflected and then absorbed solar radiation, these brightness values were converted into values of albedo. This was accomplished by comparing adjusted values of brightness at selected 5° latitude-longitude grid points with estimates of albedo derived by the author from Nimbus 2 measurements under assumption of diffuse reflection and from aircraft observations (Roach 1961). These comparisons were made over the same or similar parts of the earth's surface or over similar cloud cover. Cases chosen consisted of measurements over cloudless ocean, vegetated terrain, desert, snow, and bright overcast cloudiness. The Nimbus albedo values were from June 1966, while Roach's measurements were made in various months during 1958–60. These albedo values are plotted as a function of ESSA 5 brightnesses during June 1967 in figure 1. A simple linear relationship, which was fitted by eye to these data, is also shown. The equation for this line is

$$\alpha = 5.49b + 8.20 \qquad (1)$$

where b is adjusted brightness on a zero to ten scale and α is albedo in percent. It will be noted that the albedo

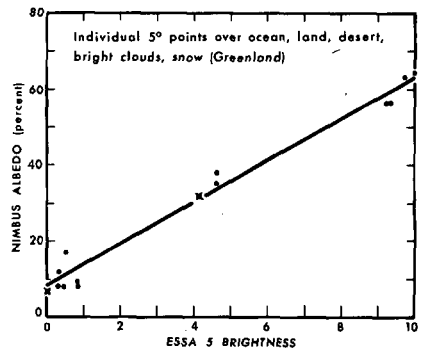

FIGURE 1.—Relationship between albedo from Nimbus 2 data (dots) and aircraft observations (Xs) and brightness from ESSA 5 pictures. Data are for different years, but over similar reflecting surfaces. Nimbus and ESSA values are averages over 5° latitude-longitude squares. Albedo values were derived under the diffuse assumption. The straight line indicates relationship used to convert brightness values into albedo.

is thus constrained between limits of 8.20 and 63.10 percent, but these appear to be reasonable minimum and maximum values, especially since they apply to averages for a 5° latitude-longitude grid.

Admittedly the diffuse assumption is a very simple one and studies of angular dependence in TIROS measurement by Ruff et al. (1968) and Arking [3] and in aircraft measurements by Cherrix and Sparkman (1967), Bartman (1967), and Salomonson (1968) do indicate substantial deviations from isotropy for certain types of clouds and surfaces, particularly for lower solar elevations. Using such information, Raschke and Bandeen (1970) formulated a universal angular law and applied it in their derivation of albedo from the Nimbus 2 measurements. It turns out, of course, that differences in albedo values obtained by assuming diffuse reflection on the one hand and through angular adjustments on the other hand are almost negligible except at latitudes where the minimum solar zenith angle for the day is more than about 50°–60°. For places with low sun all day, albedos based on the Raschke-Bandeen law were as much as one-third greater than values derived under the diffuse assumption from the Nimbus measurements (e.g., the interior of Greenland had a maximum albedo of about 80 percent in the Raschke-Bandeen charts whereas maximum diffuse values are about 60 percent). This means that the meridional gradients of albedo (between high and low latitudes), and absorbed solar radiation derived therefrom, are somewhat greater than those obtained using the diffuse assumption. Unfortunately, even if a satisfactory angular law could have been devised for the ESSA picture data, lack of the necessary angular informa-

[2] All digitized brightness values on the archival tape since Feb. 1, 1967 have been "normalized" to overhead sun (i.e., each original digitized value was divided by the cosine of the solar zenith angle of the viewed spot). Thus all brightness values referred to in this paper have already been normalized.

[3] Arking, A., "The Angular Distribution of Scattered Solar Radiation and the Earth Albedo as Observed from TIROS", presented at the Symposium on Atmospheric Radiation, International Association of Meteorology and Atmospheric Physics (IUGG), Leningrad, U.S.S.R., August 1964.

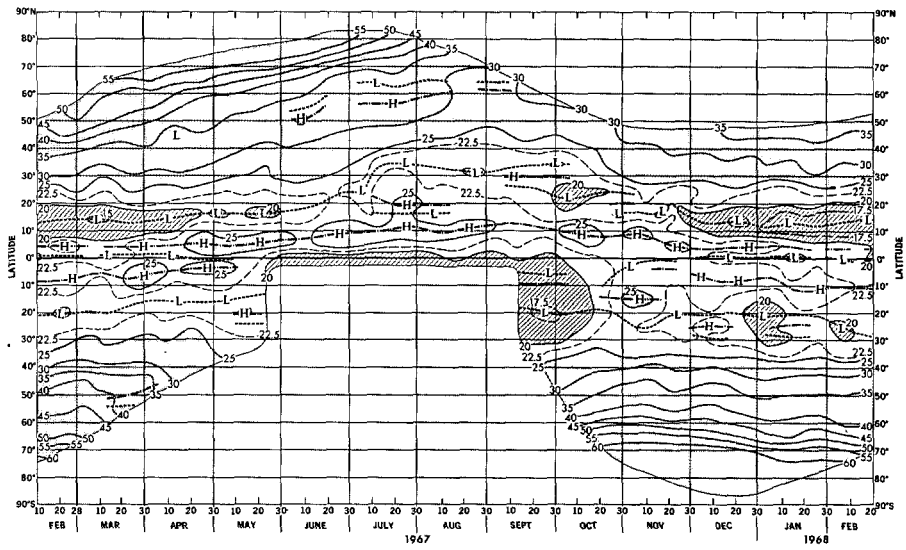

FIGURE 2.—Annual course of zonal mean albedo (percent) based on 6-day mean values from ESSA 3 and 5 digitized brightness. Values less than 20 percent are hatched, greater than 25, stippled. Dashed lines mark minima and dot-dashed lines maxima in the meridional direction, so indicated only for those lasting at least 2 consecutive 6-day periods. H and L indicate maxima and minima, respectively, in both latitude and time. Unanalyzed areas had unreliable data or no sunlight.

tion in the archive effectively constrained us to the use of the diffuse assumption in making albedo estimates.

The other major assumption made in estimating planetary albedo and absorbed solar radiation from these data is that a single midafternoon brightness observation (local time approximately 1400–1600 for ESSA 3 and 5 pictures) is meteorologically representative of the whole day. This may be poor where weather systems are undergoing rapid changes or where marked diurnal variations in daytime cloudiness occur. The former effect is generally not too serious since we are considering only zonal means of 5° latitude-longitude averages. The diurnal effect is certainly of some importance over land areas; afternoon brightnesses observed over land areas where convective activity is present may yield albedos that are biased toward the high side. Again, since only large-scale zonal means are being considered here, such a bias is probably of relatively little consequence.

The mean absorbed solar radiation for each latitude each day was obtained by multiplying the available solar radiation by one minus the zonal mean albedo. A solar constant of 1.95 ly/min (0.136 $J \cdot cm^{-2} \cdot s^{-1}$) (Laue and Drummond 1968, Stair and Ellis 1968) was used in calculating the available solar radiation for the particular latitude and day.

Nonoverlapping 6-day averages of zonal mean albedo and absorbed solar radiation at each 5° latitude were constructed to provide convenient portrayal of the annual course of these quantities. In addition, for further smoothing in the ensuing illustrations, weighted (binomial 1:2:1) running means of three consecutive 6-day periods were obtained. The choice of 6 days, rather than the more customary 5 days, for medium-period averaging was essentially dictated by the character of the ESSA picture data. Pronounced oscillations of 2 and 3 days were found in the ESSA 3 and 5 data, respectively, when time plots of daily 5° latitude-longitude values of brightness over deserts and snow-covered regions were examined. These oscillations were most pronounced for cases with few or no clouds and were virtually obscured when cloudiness occurred. They arose because of varying brightness over the individual picture frames, mostly in the west-east direction. This was a variation that was not eliminated by the various procedures employed to provide a uniform brightness response over the pictures before final digitizing. The variation may have been related to the nonisotropic reflectivity associated with various satellite viewing angles relative to the sun, but there is doubt that this was the sole cause of the problem; in fact, a fully acceptable explanation for it has not as yet been found. The particular periods of these oscillations corresponded to the number of days required for the orbital position of each satellite to come back in phase and traverse nearly the same path across the earth. (The earth's daily rotational period was not a multiple of the satellites' orbital periods.) Even though these oscillations were not large enough to obscure basic changes in brightness due to changes in cloudiness and snow cover, it seemed desirable to choose a medium-scale time period of averaging which would tend to eliminate these 2- and 3-day oscillations. Averaging over 6 days was, therefore, an obvious choice.

3. ANNUAL COURSE OF ZONALLY AVERAGED ALBEDO

A broadscale view of zonal mean albedo derived from more than a year of the digitized picture data is given

in figure 2, where the annual course of albedo is portrayed in more detail than ever before possible at a large number of latitude circles. Figure 2 is dominated by the very large-scale features that are characteristic of the meridional profiles of albedo that have been derived from somewhat more limited amounts of satellite radiometer data (Bandeen et al. 1965, Winston 1969, Raschke and Bandeen 1970); that is, higher values of albedo at higher latitudes of both hemispheres; a secondary maximum near, but mainly north of, the Equator; and lower values in the Tropics and subtropics of both hemispheres. The data and representation of figure 2, however, give a clear portrayal of the seasonal, monthly, and shorter period variations of the zonal mean albedo. In view of the lack of comparable data from other years, those variations that are purely climatological cannot be separated from the anomalous variations for this particular year. In any event, let us examine the variations of these major features of the albedo through most of 1967 and the early part of 1968.

The maximum of albedo associated with the intertropical convergence zone. Virtually all year there is a clearcut maximum albedo north of the Equator varying in latitudinal position from 3°–7°N in winter and spring to 10°–12°N in summer and autumn. The major shift northward to 10°–12°N occurs in late May and June and the major return southward occurs abruptly in November. Note that, in late July–early August, values nearly as high extend northward to 20°–25°N with a weak secondary maximum in evidence, largely associated with the farthest northward penetration of monsoon cloudiness over Southeast Asia. In the period December–early May, a maximum is also found south of the Equator between 3° and 12°S. Values in this southern maximum zone are generally higher than in the zone north of the Equator and this maximum is also generally broader meridionally in the periods when the two zones coexist. Neither maximum axis crosses the Equator, but instead a distinct, although sometimes weak, minimum occurs between them at the Equator.

The subtropical minimum in the Northern Hemisphere. This minimum is most pronounced from November to May between latitudes 10° and 20°N. In June it shifts gradually northward of 20°N and then about July 10 moves abruptly to near 35°N, remaining between 30° and 35°N through the summer. The southward retreat of this minimum in the fall occurs in a series of discontinuous shifts, new minima being established about 10° farther south in September and again in late October, with subsequent fading away of the more northerly minima.

The subtropical minimum in the Southern Hemisphere. This minimum, which hovers at 20°S in February and March 1967, drifts gradually northward through late May and presumably remains at its most northerly position throughout the Southern Hemisphere winter. In September, the major minimum axis is farther south again and remains between about 18° and 26°S throughout the remainder of the period, except for the southward shift in February 1968 to a position well south of that in February 1967. In general, during the period from September to January this minimum is more diffuse than it is in the first third of 1967 and also more diffuse than the corresponding minimum in the Northern Hemisphere throughout most of the year.

The increases in albedo poleward from the major subtropical minima. Over most of the year for which data are adequate, the poleward increase of albedo is monotonic. The principal exception occurs over the Northern Hemisphere in summer when a weak minimum is found frequently between about 55° and 65°N and an accompanying weak maximum occurs between 50° and 60°N. This minimum is located just south of most of the remaining polar ice cap and north of the cloudiness associated with the major storm track for summer that forms a maximum near the northern limit of the temperate zone. During the remainder of the year, the increasing cloudiness northward through middle latitudes merges with the Arctic ice and snow cover to produce the continuous rise in albedo toward the North Pole.

For the warm season in the Southern Hemisphere there is virtually no comparable interference with the monotonic increase poleward, although there is a marked decrease in gradient of albedo northward of the intense gradient near 60°–70°S that largely marks the edge of the Antarctic ice. There is a secondary maximum in the gradient of albedo between about 35° and 50°S that is associated with the north side of the major cloudiness of temperate latitudes. This gradient undergoes some marked variations in intensity in November through January whereas the gradient near Antarctica exhibits mainly the type of gradual shift southward that is to be expected as the ice retreats during the southern summer.

Over the Northern Hemisphere, the gradient southward from the polar regions also has two maxima between February and July 1967. The more northerly maximum displays a very pronounced northward drift from 40°–50°N in February and March 1967 to north of 70°N by July. To a great extent, this drift must be associated with the gradually retreating snow and ice over the continents and polar seas, but location of the maximum in middle latitudes in winter is also related to northward increases in cloudiness over both oceans and continents. That this gradient did not reappear in the following winter is interesting. The ESSA 3 camera was apparently not responding adequately at higher latitudes in the fall and winter of 1967–68 and even as far south as 40°N the data may be biased toward low values. However, examination of particular areas over Asia and North America that appeared to be snow covered in both years indicates that brightness values in these locations were about the same in the two years. So it is likely that there *was* less snow and cloudiness in middle latitudes in February 1968 than in February 1967.

The maximum gradient of albedo at the southern edge of the temperate zone cloudiness in the Northern Hemisphere is generally quite pronounced in the period February–April 1967 between latitudes 20° and 35°N. In late spring and summer it weakens and shifts northward, reaching 40°–50°N by early August. After remaining very narrow and weak during late summer and autumn, it strengthens and is again located between 20° and 35°N in December 1967–February 1968.

Obviously, the meridional shifts and temporal variations of these features signify certain temporal variations of the albedo at each latitude. The annual cycle stands out clearly northward from latitude 30°N, with minimum values in late summer and maximum values in winter or spring. At latitudes 10°–20°N, the phase of the annual variation is reversed, with maximum values in summer and minimum values in winter. At latitudes 0°–5°N, the phase of the annual variation reverses again, but the amplitude is smaller and there appears to be more influence of semiannual and shorter oscillations. At latitudes 20° and 25°N, where the subtropical minimum passes through in early summer and again in fall, the annual cycle is weaker and more of a semiannual or shorter variation is dominant. Further analysis of the various time variations will be made in the next section.

Since there are distinctive variations in albedo within latitude circles (cf. Winston 1967, Taylor and Winston 1968), it was decided to examine also the annual course of albedo averaged over each of three component zones, 120° longitude in width. These zones roughly encom-

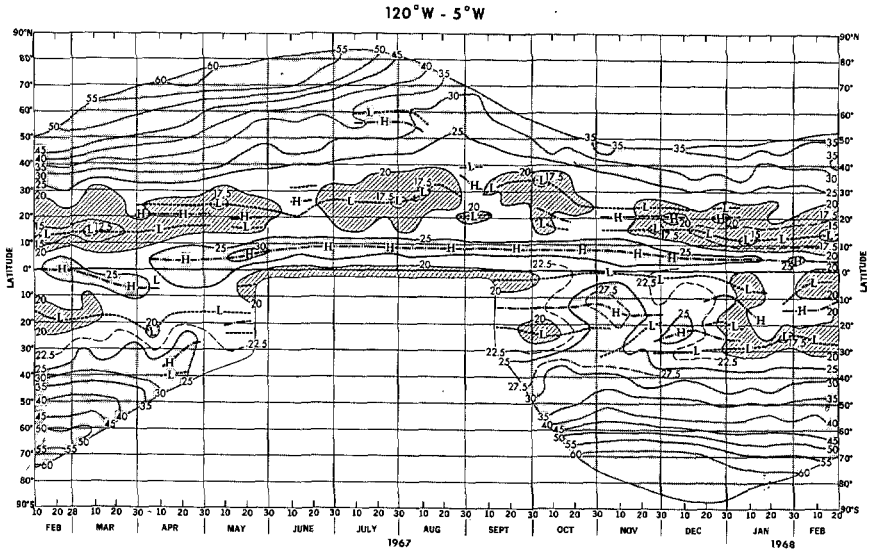

FIGURE 3.—Annual course of zonal mean albedo (percent) based on 6-day mean values from ESSA 3 and 5 brightness for the sector 120°–5°W. See caption to figure 2.

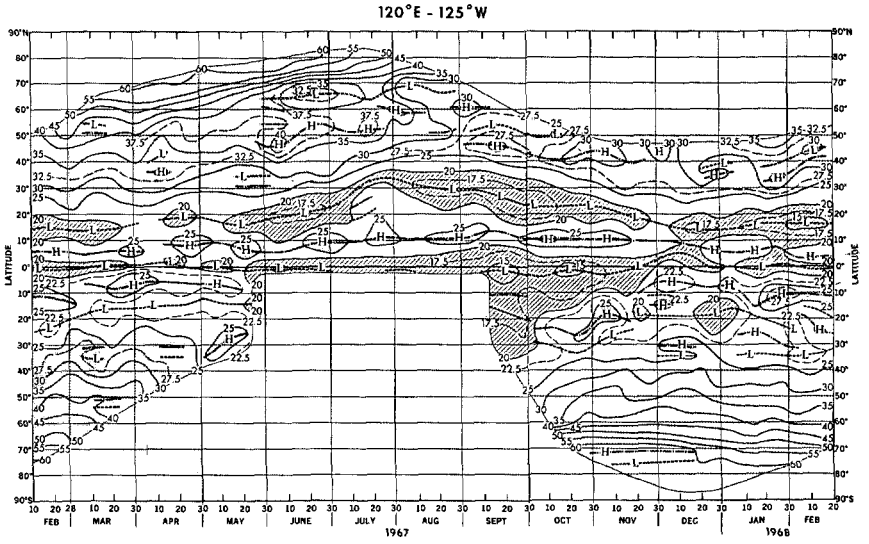

FIGURE 4.—Same as figure 3 except sector 120°E–125°W.

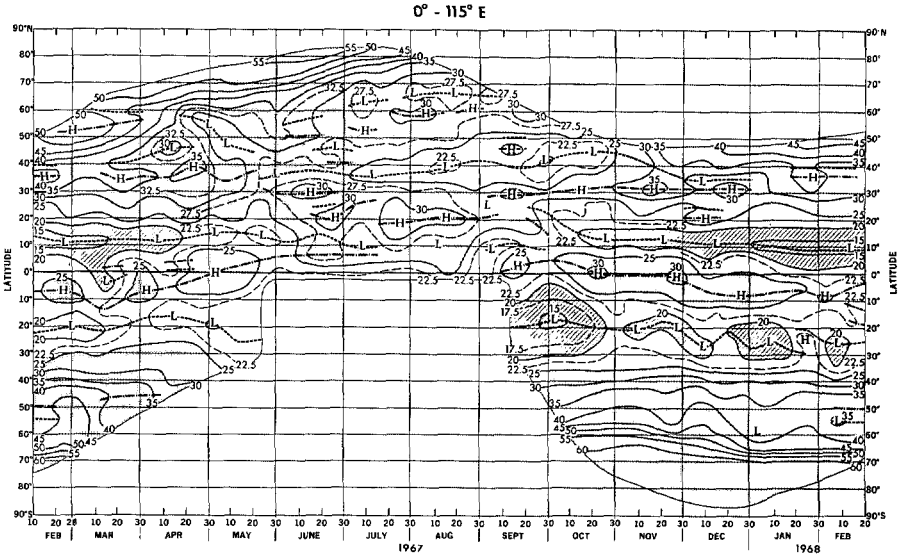

FIGURE 5.—Same as figure 3 except sector 0°–115°E.

pass the Atlantic Ocean and the Americas (120°–5°W), the Pacific Ocean (120°E–125°W), and Eurasia, Africa, and the Indian Ocean (0°–115°E). The annual course of the component zonal mean albedo in each of these zones is shown in figures 3–5.

It is immediately apparent that the patterns for the two predominantly oceanic zones (120°–5°W and 120°E–125°W) strongly resemble that of the overall zonal mean, whereas the annual course for the largely continental zone of 0°–115°E exhibits the greatest differences from that of the overall mean. The latter is not too unexpected in view of the large-scale influence of the monsoonal variations over Asia and the Indian Ocean. It is notable in figure 5 how the rapid increase in albedo in the first half of June between 5° and 30°N seems to completely obliterate the previously existing pattern of minimum albedo at 10°–15°N and maximum albedo between 10°S and 5°N. With the termination of the summer monsoon in September, this pre-existing tropical pattern resumes almost as rapidly as it disappeared in June.

Also unique in this zone (0°–115°E) is the pronounced minimum of albedo that becomes strongly established near 35°N by July and maintains well into the fall season. This zone too is the only one where the maximum of albedo associated with the intertropical convergence zone can be clearly traced across the Equator, northward in April-May and southward in October-November. In the latter period, it pauses over the Equator for a whole month before shifting more rapidly southward in December. This zone is also notable for a strong, subtropical minimum of albedo in the Southern Hemisphere which has clearcut continuity through virtually all of the period shown in those latitudes.

In the Pacific zone (fig. 4) twin tropical maxima of albedo north and south of the Equator are prevalent most of the time from February to May and from November to February. As pointed out by Hubert et al. (1969), the western Pacific is the only location where a double axis of tropical cloudiness is found on the seasonal mean global brightness charts (for this same year). The Atlantic zone (fig. 3) predominantly exhibits a single zone of maximum albedo with least variation in intensity and latitudinal position. With the interesting exception of February to early April 1967, it remains fixed between about 2° and 10°N. In general, this zone has the simplest overall pattern of albedo variation.

4. HARMONIC ANALYSIS OF TIME VARIATIONS OF ZONAL MEAN ALBEDO

In describing the features of the annual course of the mean zonal albedo, the prevalence of certain large-scale temporal oscillations in albedo at various latitude circles was noted. To more readily and objectively assess the relative importance of these annual, semiannual, and shorter period variations, the time series of zonal mean values at various latitude circles were subjected to harmonic analysis. Daily zonal mean values at each 5° latitude circle between 0° and 45°N (i.e., where coverage was complete over the whole year) were analyzed for the period February 1967–January 1968. Plots of the amplitudes of the various harmonics for frequencies 1 (365 days) to 31 (about 12 days) at each latitude are given in figure 6.

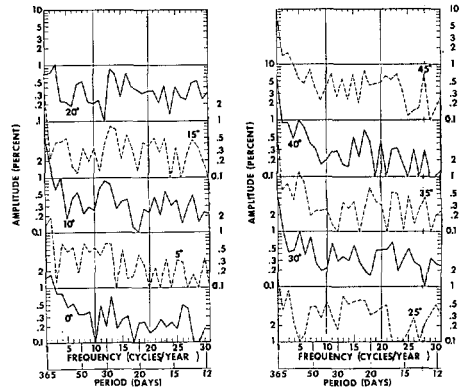

FIGURE 6.—Plots of amplitudes of albedo at latitudes 0°–45°N for various frequencies (periods), based on data from Feb. 1, 1967–Jan. 31, 1968.

The annual cycle dominates all other cycles for latitudes 25°–45°N and 10°–15°N. At 0°, 5°N, and 20°N, the semiannual cycle is a bit stronger than the annual. At 20°N, however, frequency 3 has a slightly larger amplitude than either frequency 1 or 2. Beyond these three very low frequency oscillations (frequencies 1–3) there are only a relatively few amplitudes that stand out consistently at two or more adjacent latitudes. For example, frequency 4 (91 days) is rather pronounced at latitudes 0°–10°N and frequency 5 (73 days) is very clearcut at latitudes 35°–40°N.

At a more intermediate scale, there is a strong preference for a maximum amplitude at frequency 12 or 13 (28–30 days) between latitudes 0° and 20°N. At most of these latitudes, the amplitude for this 28–30-day oscillation is bigger than the amplitude for any period except that of the very low frequencies (1–4). There is some tendency for a maximum at frequency 12 or 13 at latitudes 25°–45°N, but it does not stand out from other similar undistinguished maxima. Thus, this 28–30-day oscillation in albedo seems to be favored in the Tropics and subtropics of the Northern Hemisphere. Interestingly enough, this period is approximately that of the lunar cycle, which has been found frequently in recent years in connection with rainfall and other parameters (cf. Bradley et al. 1962, Brier and Bradley 1964, Lund 1965). As might be expected, analysis of brightness data for some particular locations in the Tropics over part of 1967 has shown a peak amplitude for this same 28–30-day period and also for the period of 14 to 15 days, the semilunar period (private communication from G. Brier). Note in figure 6 that the amplitude of frequency 26 (14.0 days) is almost as prominent as frequency 13 at the Equator, but this same period exhibits relatively little prominence at most other latitudes. However, frequency 25 (14.6 days) shows a max-

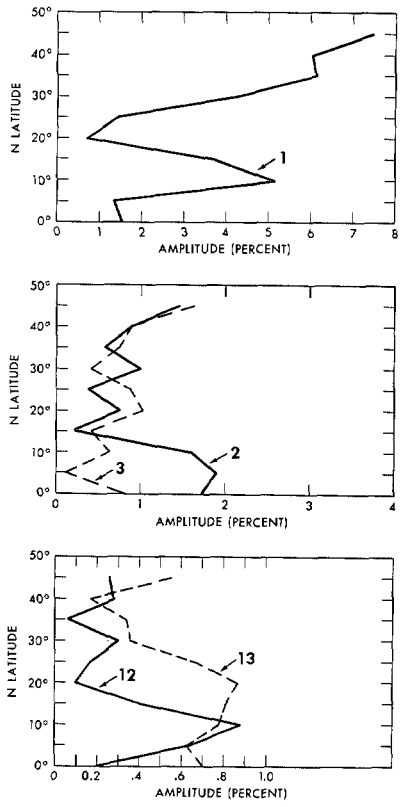

FIGURE 7.—Variation of amplitude of albedo with latitude for very long periods (frequencies 1–3) and for 28–30-day periods (frequencies 12 and 13).

imum at several latitudes, but in general it is not a maximum that is clearly distinguishable from several other maxima for other frequencies between 20 and 29.

For some of the more prominent frequencies just cited, variations of amplitude with latitude can be more easily examined in figure 7. Thus, for the annual cycle, the peak at 10°–15°N stands out clearly with much smaller amplitudes both near the Equator and in the subtropics. The amplitudes in middle latitudes (from 30°N northward) are also large. The largest amplitudes of frequency 2 occur between 0° and 10°N while frequency 3 has a maximum at 20°N where both frequencies 1 and 2 are small. The latitudinal predominance of frequency 12 at 5°–15°N is quite clear, while frequency 13 maintains relatively high values at 0°–25°N with considerably weaker values at 30°–40°N. Thus, oscillations of the 28–30-day period are prominent from the Equator through the subtropics of the Northern Hemisphere, both in comparison with latitudes farther north (except possibly 45°N) and with oscillations of other periods within these lower latitudes.

5. ANNUAL COURSE OF ABSORBED SOLAR RADIATION

The foregoing variations in the albedo are of interest in their own right since they are principally manifestations of varying cloudiness and snow cover. However, their influence on the energetics of the earth-atmosphere system must always be considered through their superposition on the strong solar heating cycle imposed by the existing astronomical relationships. Thus, it is useful to exhibit the distribution of absorbed solar radiation that is prescribed by the albedo values represented in figure 2. The latitude-time distribution of 6-day mean values of this absorbed solar radiation is shown in figure 8. A strong annual cycle poleward of the subtropics in the Northern Hemisphere (and also in the Southern Hemisphere as far as can be seen in figure 8) and the tendency toward a semiannual cycle near the Equator are, of course, quite dominant since the relative variations in the available solar energy are much larger than those of the albedo.

At latitudes 20°–45°N, the annual minimum of absorbed solar radiation occurs very close to the December solstice since the minimum in the available solar energy is quite pronounced (see table 134, p. 419, List 1963) and the albedo has relatively small temporal variations during this part of the year. On the other hand, the available solar energy has a rather broad maximum in summer so that temporal variations in albedo have a noticeable impact. Thus, the fact that the minimum albedo for the year occurs at many of the temperate and polar latitude circles of the Northern Hemisphere in late summer tends to delay the year's maximum absorbed radiation until July (e.g., July 15–20 at 30°–40°N). The energy absorbed at the delayed maximum amounts to about 5 percent more than the absorbed energy at the solstice at latitudes 30°–45°N and about 10 percent more at 70°–90°N, but the difference is negligible at other latitudes.

The continuing low values of albedo in the early fall relative to early spring, northward from 20°N, tend to disturb further the overall symmetry of the absorbed solar radiation with respect to the summer solstice. Thus, its gradient with time in fall and its ascendant in spring are both delayed relative to the equinoxes, whereas the temporal ascendant and gradient of the available solar energy are nearly equal at the two equinoxes (see again table 134, p. 419, List 1963). The contrasts in the meridional distributions of albedo and absorbed solar radiation at the vernal and autumnal equinoxes for the Northern Hemisphere are illustrated clearly in figure 9, where profiles for the two 6-day periods closest to the equinoxes are shown. The consistently higher values of albedo at all latitudes from 20°N northward in March relative to September result in markedly lower values of absorbed solar radiation at the vernal equinox; values average about 0.05 ly/min less between 25° and 60°N. Since the albedo at 10°–15°N is lower in March than in September, the overall contrast in heating between the Tropics and high latitudes is considerably stronger at the vernal equinox. Only north of 35°N are the poleward heating gradients comparable for the two periods.

It is interesting that the maximum absorbed solar radiation in summer in the Southern Hemisphere is more uniform and more nearly symmetrical about the solstice than in the Northern Hemisphere. There is only a slight lag in the maximum relative to the solstice at most latitudes

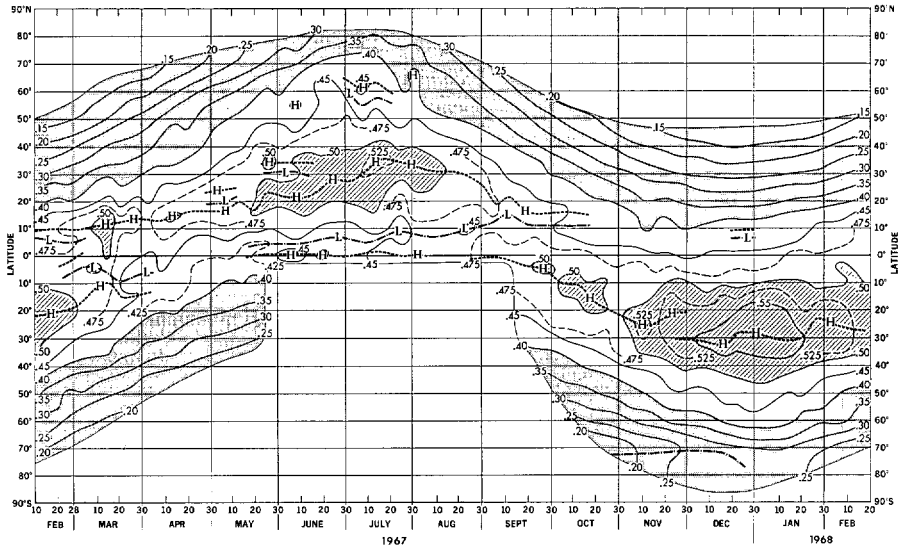

FIGURE 8.—Annual course of zonal mean absorbed solar radiation (ly/min) based on 6-day mean albedo values and available solar energy at top of atmosphere. Values less than 0.40 ly/min are stippled, greater than 0.50, hatched. Dashed lines mark maxima and dot-dashed lines, minima in the meridional direction, so indicated only for those lasting at least two consecutive 6-day periods. H and L indicate maxima and minima, respectively, in both latitude and time. Unanalyzed areas had unreliable data or no sunlight.

from the Tropics southward; generally the maximum radiation is absorbed about January 1. The location of the maximum of absorbed solar radiation for the Southern Hemisphere near latitude 30° in summer is fairly similar to the Northern Hemisphere, but the major maximum seems to reach this latitude sooner relative to the solstice than in the Northern Hemisphere. South of 55°S near the southern summer solstice the considerably higher values of albedo maintain the absorbed energy at a level lower than the absorbed energy north of 55°N near the northern summer solstice. Thus, the general tendency of the absorbed energy in southern summer to be higher than in northern summer because of the shorter distance from earth to sun is reversed at these high latitudes. Note that the effect of the earth–sun distance is appreciable in temperate and subtropical latitudes of the Southern versus the Northern Hemisphere in summer and that the difference is even accentuated a bit by the generally lower albedos in southern summer as compared with northern summer, at subtropical latitudes (fig. 2). In combination, all of these differences between absorbed solar radiation in the two hemispheres near the two summer solstices signify that the differential heating between subtropics and higher latitudes in the southern summer is substantially greater than that in the northern summer. An example of these differences is illustrated clearly by the meridional profiles of albedo and absorbed solar radiation for two 6-day periods centered about 10 days after the summer solstice in each hemisphere (fig. 10).

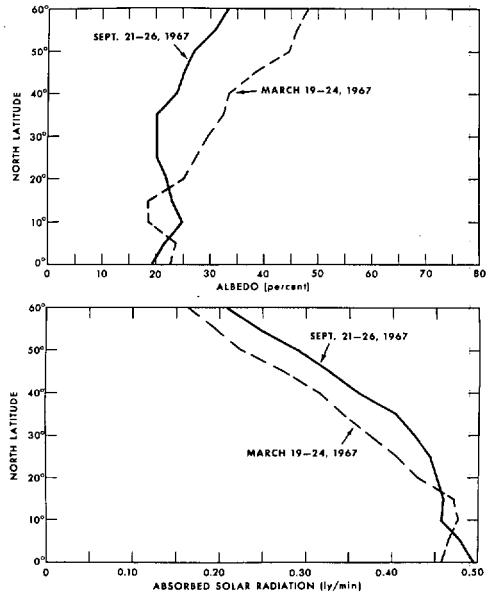

FIGURE 9.—Contrasting profiles of zonal means of albedo (top) and absorbed solar radiation (bottom) near times of vernal and autumnal equinoxes.

6. CONCLUSIONS

These first detailed representations of the annual course of zonal mean albedo and absorbed solar radiation surely reveal much of what is normally characteristic of the effects of variations in cloudiness and ice and snow over the year on the annual cycle of solar energy available to the earth-atmosphere system. Very complete longitudinal coverage around the various latitude circles makes these data especially valuable for giving a reliable picture of what variations in the zonally averaged albedo are really like. The next step, however, is to examine the

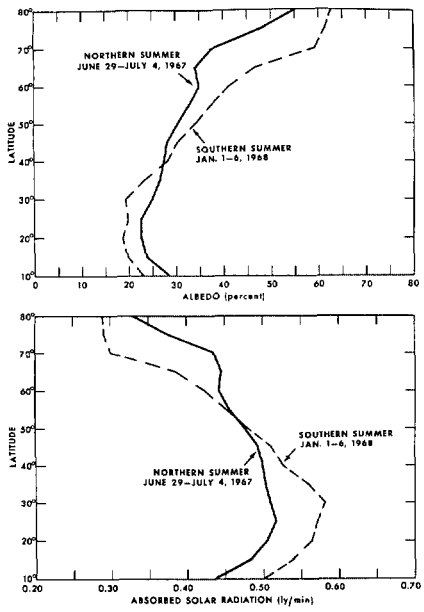

FIGURE 10.—Same as figure 9 except periods shortly after the summer solstice of Northern and Southern Hemispheres.

annual course of zonal mean albedo for additional years so that determinations of the normal and deviations therefrom can be made. Accurately detecting year-to-year differences in albedo using picture brightness is difficult and depends on how well the data can be normalized to a uniform response to true reflected solar energy. Examination of digitized data subsequent to the sample used in this study indicates that, although several months of data in portions of 1968–70 will probably not be amenable to compatibility adjustments, a major portion of the data through 1970 will be. It is hoped that the annual course of zonal mean albedo for at least one of these more recent years can be constructed and meaningfully compared with the annual course for 1967–68 shown here.

Looking beyond picture data, more satisfactory determination of albedo is anticipated from the visible channel of the two-channel scanning radiometer which has become a standard part of the instrumentation of operational environmental satellites (beginning with ITOS 1). Routine accumulation of quantitatively reliable data on reflected solar energy should enable us to investigate much more fully the temporal and spatial variations of albedo of the earth-atmosphere system. In addition, the infrared channel of the same operational two-channel radiometer should permit similar routine accumulation of reliable data on the other component of the earth-atmosphere radiation budget—the outgoing longwave radiation.

ACKNOWLEDGMENTS

I wish to thank several present and former members of the Office of Research of the National Environmental Satellite Service for their contributions to this study: Dr. T. Murakami for his assistance and advice with respect to the harmonic analysis of albedo data from the original brightness archive, Mr. C. R. Earnest and Miss B. Mengel for their assistance with computer calculations, Mr. J. J. Hildebrand for computational help and other general assistance with the data, and Mrs. M. Varnadore and Mr. L. D. Hatton for their painstaking work in drafting the figures.

REFERENCES

Bandeen, William R., Halev, M., and Strange, I., "A Radiation Climatology in the Visible and Infrared From the TIROS Meteorological Satellites," *NASA Technical Note* No. D–2534, National Aeronautics and Space Administration, Washington, D.C., June **1965**, 30 pp.

Bartman, Fred L., "The Reflectance and Scattering of Solar Radiation by the Earth," *Technical Report*, Contract No. NASr–54(03), Department of Aerospace Engineering, University of Michigan, Ann Arbor, Feb. **1967**, 257 pp.

Booth, Arthur L., and Taylor, V. Ray, "Meso-Scale Archive and Computer Products of Digitized Video Data From ESSA Satellites," *Bulletin of the American Meteorological Society*, Vol. 50, No. 6, June **1969**, pp. 431–438.

Bradley, Donald A., Woodbury, Max A., and Brier, Glenn W., "Lunar Synodical Period and Widespread Precipitation," *Science*, Vol. 137, No. 3532, Sept. 7, **1962**, pp. 748–749.

Brier, Glenn W., and Bradley, Donald A., "The Lunar Synodical Period and Precipitation in the United States," *Journal of the Atmospheric Sciences*, Vol. 21, No. 4, July **1964**, pp. 386–395.

Bristor, C. L., "Computer Processing of Satellite Cloud Pictures," *ESSA Technical Memorandum* NESCTM–3, National Environmental Satellite Center, Suitland, Md., Apr. **1968**, 11 pp.

Bristor, C. L., Callicott, W. M., and Bradford, R. E., "Operational Processing of Satellite Cloud Pictures by Computer," *Monthly Weather Review*, Vol. 94, No. 8, Aug. **1966**, pp. 515–527.

Cherrix, G. T., and Sparkman, B. A., "A Preliminary Report on Bidirectional Reflectances of Stratocumulus Clouds Measured With an Airborne Medium Resolution Radiometer," *Report* X–622–67–48, Contract NASA–TM–X–55659, Goddard Space Flight Center, National Aeronautics and Space Administration, Greenbelt, Md., Feb. **1967**, 33 pp.

Hubert, L. F., Krueger, A. F., and Winston, J. S., "The Double Intertropical Convergence Zone: Fact or Fiction?," *Journal of the Atmospheric Sciences*, Vol. 26, No. 4, July **1969**, pp. 771–773.

Kornfield, Jack, and Hasler, A. Frederick, "A Photographic Summary of the Earth's Cloud Cover for the Year 1967," *Journal of Applied Meteorology*, Vol. 8, No. 4, Aug. **1969**, pp. 687–700.

Laue, E. G., and Drummond, A. J., "Solar Constant: First Direct Measurements," *Science*, Vol. 161, No. 3844, Aug. 30, **1968**, pp. 888–891.

List, Robert J., *Smithsonian Meteorological Tables*, 6th Revised Edition, Smithsonian Institution, Washington, D.C., **1963**, 527 pp.

Lund, Iver A., "Indications of a Lunar Synodical Period in United States Observations of Sunshine," *Journal of the Atmospheric Sciences*, Vol. 22, No. 1, Jan. **1965**, pp. 24–39.

Raschke, E., and Bandeen, William R., "The Radiation Balance of the Planet Earth From Radiation Measurements of the Satellite Nimbus II," *Journal of Applied Meteorology*, Vol. 9, No. 2, Apr. **1970**, pp. 215–238.

Rasool, Ishtiag, and Prabhakara, C., "Heat Budget of the Southern Hemisphere," *Papers of the 6th International Space Science Symposium, Mar del Plata, Argentina, May 11–19, 1965, Problems in Atmospheric Circulation*, Spartan Books, Washington, D.C., **1966**, pp. 76–92.

Roach, W. T., "Some Aircraft Observations of Fluxes of Solar Radiation in the Atmosphere," *Quarterly Journal of the Royal Meteorological Society*, Vol. 87, No. 373, London, England, July **1961**, pp. 346–363.

Ruff, I., Koffler, R., Fritz, S., Winston, J. S., and Rao, P. K., "Angular Distribution of Solar Radiation Reflected From Clouds as Determined From TIROS IV Radiometer Measurements," *Journal of the Atmospheric Sciences*, Vol. 25, No. 2, Mar. **1968**, pp. 323–332.

Salomonson, Vincent V., "Anisotropy in Reflected Solar Radiation," *Atmospheric Science Paper* No. 128, Department of Atmospheric Science, Colorado State University, Ft. Collins, Aug. **1968**, 143 pp.

Schwalb, Arthur, and Gross, James, "Vidicon Data Limitations," *ESSA Technical Memorandum* NESCTM 17, National Environmental Satellite Center, Suitland, Md., June **1969**, 22 pp.

Stair, Ralph, and Ellis, Howard T., "The Solar Constant Based on New Spectral Irradiance Data From 310 to 530 Nanometers," *Journal of Applied Meteorology*, Vol. 7, No. 4, Aug. **1968**, pp. 635–644.

Taylor, V. Ray, and Winston, Jay S., "Monthly and Seasonal Mean Global Charts of Brightness From ESSA 3 and ESSA 5 Digitized Pictures, February 1967–February 1968," *ESSA Technical Report* NESC 46, National Environmental Satellite Center, Washington, D.C. Nov. **1968**, 9 pp. and 17 charts.

Vonder Haar, Thomas H., "Variations of the Earth's Radiation Budget," Ph. D. thesis, Department of Meteorology, University of Wisconsin, Madison, Feb. **1968**, 118 pp.

Winston, Jay S., "Planetary-Scale Characteristics of Monthly Mean Long-Wave Radiation and Albedo and Some Year-to-Year Variations," *Monthly Weather Review*, Vol. 95, No. 5, May **1967**, pp. 235–256.

Winston, Jay S., "Global Distribution of Cloudiness and Radiation as Measured From Weather Satellites," *World Survey of Climatology*, Vol. 4, *Climate of the Free Atmosphere*, Elsevier Publishing Co., Amsterdam, The Netherlands, **1969**, pp. 247–280.

[*Received December 28, 1970; revised February 26, 1971*]